ORIGINAL PAPER

Sébastien Michel[ID]

Part-through cracks computation in an Euler–Bernoulli beam model

© The Author(s) 2023

Abstract The reduction of the equations of a slender, brittle continuum to a one-dimensional theory and the possibility of accounting for the cracking of this body has received much attention recently. This contribution investigates the effect of cross-sectional geometry on damage localization in an Euler–Bernoulli beam. Two geometric fields characterizing the crack penetration depth on each side of the beam are introduced, from which the modulation of the bending and tensile parts of the strain energy by the crack depth is deduced. The geometry of the crack-tip envelope is obtained by energy minimization. We find that in the case of a Griffith-like dissipation potential, the characteristic size of the crack is a key element for predicting initiation at a finite external load. We can accurately predict the initiation position by regularizing the model in the spirit of Variational Brittle Fracture. Model predictions are compared against computational results obtained by the classical damage field theory.

1 Introduction

1.1 Motivation

Finding how and when cracks develop in a 3D continuum has immediate relevance in applications. The seminal paper of Griffith [1] rooted the problem in an energetic framework where crack development is driven by the competition between the elastic energy stored within the deforming body and the crack energy. Formulation in the modern variational framework was only achieved recently [2] and pinpointed the troubles of Griffith's theory to handle initiation [3–5]. The need for numerical implementation lead to the development of phase-field models [6,7]: a damage field modeling the phase transition of the material from pristine to damaged is introduced and regularized by the addition of higher gradients. Refinements allow to mimic various material behavior [8–10], and the framework proves successful for describing the crack initiation and propagation in many situations [11] - see for example [12] for a review.

A beam theory requires describing the behavior of each section associated with a position on a centre-line, a geometric abstraction grasping the shape of a slender body. For some geometries, the loads result in a tensile stress all over the sections, legitimating the use of the brittle assumption [13,14]. When bending is included, the non-zero yet limited load-bearing capacity in tension together with the different capacities of a brittle material in tension and compression result in the preferential development of cracks on the tensiled side of the body [15,16]. This asymmetry results in significant variation of the sections characteristic geometrical quantities [17,18] and requires special care when handling the description of the beam with developed cracks [19–21]. Recent attempts at developing a phase-field theory of beams or shells [22,23] grasping the initiation of the

S. Michel (✉)

Department of Morphology and Geometric Modeling, Budapest University of Technology and Economics, Műegyetem rkp. 3, 1111 Budapest, Hungary
E-mail: sebastien.michel@edu.bme.hu

fracture stemmed from the idea that a damage field can be used to represent the crack penetration depth in the beam [24]. In [25], the shape of the damage field is postulated whereas [26] attempts at precisely describing the strain field alteration due to the existence of the cracks.

We propose here to investigate crack initiation by describing each cross section using two geometric fields measuring the crack penetration on each side of a slender body thus parametrizing the geometry of partially cracked sections. Characterizing the deformation of the sections using the Euler–Bernoulli hypothesis, we get the dependence of the bending moment in both the transversal displacement field and the geometric fields by direct integration. We formulate the problem of the equilibrium of a slender body allowed to crack in this framework, and regularize the energy functional in the spirit of the variational brittle fracture by the addition of higher gradients of the geometric fields. The solution fields are obtained as global minimizers along a time-stepping procedure. The compatibility of the minimizers with the geometric description of the body, with the irreversibility of the cracking process, and the crack localization on the tensiled side are ensured with additional constraints. From our smeared modeling, we retrieve the envelope of the crack zones in our dimension-reduced model.

1.2 Phase field modeling in $\mathbb{R}^3$

Consider a homogeneous connected body $\Omega \subset \mathbb{R}^3$ with Lipschitz boundary $\partial\Omega$. The body is in equilibrium with internal forces of density $\underline{f}_b$ and surfacic forces of density $\underline{f}_s$ whose work we will denote $\mathcal{P} = \int_\Omega \underline{f}_b \cdot \underline{u} \mathrm{d}\Omega + \int_{\partial\Omega} \underline{f}_s \cdot \underline{u} \mathrm{d}S$. Under the effect of the forces the body deforms following a displacement field $\underline{u}$ and stores energy as deformation energy of density $W(\nabla\underline{u})$. The eventual cracks of the body form a set $\Gamma \subset \mathbb{R}^2$ - supposed smooth - endowed with a surface energy of density G according to the Griffith postulate. Altogether, the total energy of the solid contains the three terms from above:

$$\mathcal{E} = \int_{\Omega-\Gamma} W(\nabla\underline{u})\mathrm{d}\Omega - \mathcal{P} + \int_\Gamma G\mathrm{d}S. \tag{1}$$

The strain energy density W is the double contraction of the strain tensor $\underline{\underline{\varepsilon}}$ with the stress tensor $\underline{\underline{\sigma}}$. Assuming small strains, the strain tensor is the symmetric part of the displacement gradient $\underline{\underline{\varepsilon}} = \frac{1}{2}(\nabla\underline{u} + \nabla\underline{u}^t)$. The main difficulty of the formulation - besides the eventual complexity of the strain energy density W - is the dependence of the functional on the unknown cracked set Γ. The elastic energy density is then given as

$$W(\nabla\underline{u}) = \frac{1}{2}\underline{\underline{\varepsilon}} : \underline{\underline{\sigma}} = \frac{1}{2}\underline{\underline{\varepsilon}} : \underline{\underline{\underline{C}}} : \underline{\underline{\varepsilon}} \tag{2}$$

The now classical method of regularization [6,7,10] consists in introducing a smooth scalar field $d : \Omega \to [0, 1]$ measuring the local degradation of the material. This field is deemed to be 0 if the material is intact and 1 wherever the material is completely destroyed $e.g$ there is no longer pressure transmission. The addition of a term depending in the scalar field gradients [7,27] ensures well-posedness for the new problem consisting of finding simultaneously the unknown displacement and damage fields [28]. A characteristic length ℓ controlling the transition size of the scalar field appears in the regularized form of the energy and can be traced with the modeling of nonlocal materials [15]. In addition, the strain energy density has to be modulated by the local value of the damage field , in order to account for the effect of the damage on the local stiffness. Physical considerations [10] and need to faithfully represent various material behavior [9] lead to different modulations of the bulk energy density. In case the load is purely tensile and the material homogeneous isotropic, a choice suggested by the reference above is $\tilde{W}(d, \nabla\underline{u}) := (1 - d)^2 W(\nabla\underline{u})$. In turn, the energy to minimize is:

$$\mathcal{E} = \int_\Omega \tilde{W}(d, \nabla\underline{u})\mathrm{d}\Omega - \mathcal{P} + G \int_\Omega \frac{d^2}{4\ell} + \ell(\nabla d)^2 \mathrm{d}\Omega. \tag{3}$$

The load dependence in time (or in some time-like control parameter) is contained in the potential energy $\mathcal{P}$. Using a gamma-convergence argument [6], one shows that the regularized energy (3) converges effectively to the original energy (1) when the characteristic length ℓ goes to zero.

In the following section, we develop an Euler–Bernoulli beam model, where the damage is characterized by the crack penetration depth. For this purpose, we follow the beam slicing into sections and specify the crack topology, on every section. In effect we retrieve a damage field whose geometric meaning is clear: it

corresponds to the crack penetration depth on each side of the beam. The stress resultants and their modulations by the crack depth are obtained by direct integration. Finally, the model is regularized by the addition of higher gradients.

2 Modeling

2.1 Material description, kinematics

In this subsection we derive from the $3D$ model (3) a $1D$ version of the penalized elastic energy density. Consider a beam, described by translating a section $[-b/2, b/2] \times [-h/2, h/2]$ along a straight line $[0, L]$, b, h and L being, respectively, the breadth, height and length of the beam. The domain occupied by the beam is $\Omega = [-b/2, b/2] \times [-h/2, h/2] \times [0, L]$. We use the frame where $\hat{z}$ points in the direction of the centre-line, and $\hat{y}$, $\hat{x}$ are in the principal directions of inertia of the section, y being the height coordinate of any point of the section. Let us associate a displacement field $w(z)\hat{y}$, deforming the centre line in its plane, and make the Euler–Bernoulli hypothesis that sections perpendicular to the centre line remain perpendicular to the centre line and deform rigidly. For a point at arclength z along the centre-line at a height y away from the neutral axis and under the small displacement assumption, the transversal displacement u is

$$u(y, z) = -w_{,z}(z)y \tag{4}$$

With our hypothesis on the displacement field and neglecting Poisson effect, only the tensile stress σ_{zz} is nonvanishing:

$$\varepsilon_{zz} = u_{,z}(y, z) = -w_{,zz}(z)y, \tag{5}$$

Consider now that the beam sections are allowed to evolve. From the Euler–Bernoulli hypotheses, the beam sections remain plane, thus we prescribe cracks to follow the beam slicing and reduce the section at particular positions. That is, we assign to each position z along the centre-line of the curve scalar fields $0 \le h^-(z)$, $h^+(z) \le h$ characterizing the damage, on each side, to each section. Effectively, we selected the damage field $d : \Omega \to [0, 1]$ appearing in (3) to be 0 in the part of the beam delimited by h^-, h^+ and 1 outside it:

$$d(x, y, z) = 1 - \mathbb{I}_{[-h/2-h^-, h/2-h^+]}(y). \tag{6}$$

where we denoted $\mathbb{I}_\Gamma(y)$ the indicator function of the set Γ, taking value 1 if $y \in \Gamma$ and 0 otherwise. To get the contribution of the damage to the bulk energy density, we start from the $3D$ formulation (3). The density of elastic energy per unit length is obtained by integrating the energy density over the beam section at position z. Taking into account our kinematic assumption (5) and our prior on the damage field (6), we get the lineic density of elastic energy for the beam:

$$\int_{-b/2}^{b/2} \int_{-h/2}^{h/2} \frac{1}{2}(1 - d)^2 \varepsilon_{zz}(z)\sigma_z z(z)\mathrm{d}y\mathrm{d}x \tag{7}$$

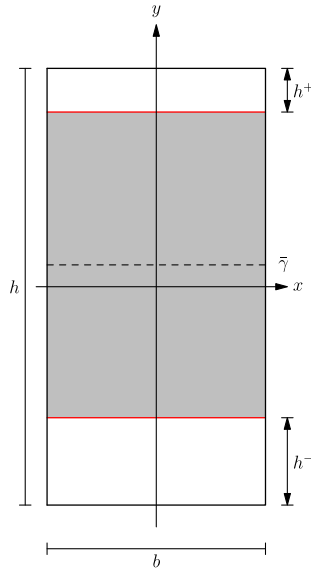$$= \int_{-b/2}^{b/2} \int_{-h/2}^{h/2} \frac{1}{2}E(1 - d)^2 \varepsilon_{zz}(z)^2 \mathrm{d}y\mathrm{d}x \tag{8}$$

$$= \int_{-b/2}^{b/2} \int_{-h/2+h^-}^{h/2-h^+} \frac{1}{2}Ew_{,zz}(z)^2 \left(y - \frac{h^- - h^+}{2} \right)^2 \mathrm{d}y\mathrm{d}x \tag{9}$$

$$= \frac{1}{2}EI(h^+, h^-)w_{,zz}(z)^2. \tag{10}$$

where the moment of inertia of the section depends on the crack penetration depths

$$I(h^+, h^-) = \frac{b}{12}(h - h^+ - h^-)^3 + \frac{b(h - h^+ - h^-)}{4}(h^- - h^+)^2 \tag{11}$$

$$= \frac{bh^3}{12} \left(1 - \frac{h^+}{h} - \frac{h^-}{h} \right)^3 + \frac{bh^3}{4} \left(1 - \frac{h^+}{h} - \frac{h^-}{h} \right) \left(\frac{h^-}{h} - \frac{h^+}{h} \right)^2. \tag{12}$$

Fig. 1 Schematics of a rectangular beam section of initial section $[-h/2, h/2] \times [-b/2, b/2]$. The undamaged part of the section is figured in gray whereas the white zones figure the cracked zones. The crack penetration depth on the top side is h^+ and on the bottom side is h^-. The centroidal line of the damaged section lies at $\overline{\gamma} = (h^- - h^+)/2$

In the second line we introduced dimensionless quantities h^+/h and h^-/h corresponding to the damaged fraction of the height of the beam section. These quantities characterize the damage to the section as damage fields: they have minimal value 0 without damage and maximal value 1 when the damage spans a whole section. They are the 1D analogous of the damage field d appearing in the first term of Eq. (3).

We now turn to the second term appearing in (3) accounting for the energy cost of creating new cracks surfaces. According to Griffith theory and in the case of a perfectly brittle material, the energy expenditure is the product of the created crack surface with the fracture toughness G. Using the fields notation we introduced above, we get that the crack energy for a crack localized at z_0 is:

$$Gbh \left(\frac{h^+(z_0)}{h} + \frac{h^-(z_0)}{h} \right). \tag{13}$$

The fundamental issue of the previous expression is that the crack is assumed to be perfectly localized at a single position z_0: the energy above does not have a density. We show in the next subsection that this results in an infinite required stress for crack propagation from a pristine material, precluding the calculation of cracks without regularization. In the next section, we include a regularization depending on the higher gradients of h^+, h^- that allow the problem to be well posed (Fig. 1).

Currently we did not introduce asymmetry in the crack development. To keep track of the side on which the crack initiation takes place, one can complexify the expression of the strain energy [29], but we find it more convenient to postpone the resolution of this issue further. As the energy minimization has to follow a time-stepping procedure, we will enforce at this latter stage the evolution of h^+, h^- depending on the sign of the curvature $w_{,zz}$. Further, note that the modulations of the sections surface and second moment of area are different for the bending part and for the tensile part, similarly to [26].

2.2 Handling the initiation

In this subsection we show that the initiation of cracks depends on the size of the mesh discretization.

Let us, just for this subsection, consider that the a crack is localized at arclength z_0 of the beam, and that this crack occupies a small portion of the beam between the arclengths $z_0 - \varepsilon/2$ and $z_0 + \varepsilon/2$ - the length ε can be taken to be a typical mesh size. Without loss of generality, due to assuming that the crack initiates on the tensiled side of the bent beam, we set $h^- \equiv 0$ and thus concern ourselves only with h^+ that we assume constant on the interval under consideration. In this setup, h^+ is a scalar parameter characterizing the crack

penetration depth in the beam element, and $0 \leq h^+/h \leq 1$ is a dimensionless parameter characterizing the crack penetration depth. Considering a Griffith-like dissipation potential, together with the results of Sect. 2.1 allows to write the energy stored in the deteriorating part of the beam

$$\mathcal{E}_\varepsilon(h^+) = \int_{z_0-\varepsilon/2}^{z_0+\varepsilon/2} \frac{EI(h^+,0)}{2} w_{,zz}^2 + \frac{Gbh}{\varepsilon}\left(\frac{h^+}{h}\right) \mathrm{d}\bar{z}. \tag{14}$$

From the Griffith criterion, the crack propagates whenever the elastic energy release rate is larger than the material toughness. Using that here the damage value h^+ is a simple scalar, the derivative of $\mathcal{E}_\varepsilon$ against h^+/h is readily computed:

$$\frac{\partial \mathcal{E}_\varepsilon}{\partial h^+} \leq 0. \tag{15}$$

Light calculations using expression (11) for $I(h^+,0)$ yields the cracking criterion at length h^+.

$$\left(-(h^+)^2 - h^+ h + \frac{h^2}{4}\right) w_{,zz}^2 \geq \frac{G}{2E\varepsilon}. \tag{16}$$

Letting h^+ go to zero, one retrieves a crack initiation criterion, determined by the geometry of the beam and the material constants:

$$w_{,zz}^2 \geq \frac{2G}{h^2 E \varepsilon}. \tag{17}$$

Crack nucleation is possible with this model only if the crack is spatially extended. That means, only smeared cracks can be computed, and the result will be more akin to a crack envelope than a localized crack. As the relapse of the bending energy is conditioned by the reduction of the section, a localized crack cannot induce the energy spending necessary for crack opening. We keep in mind this feature of the formulation, and introduce in the next section such a characteristic length.

3 Problem formulation and resolution

3.1 Regularized problem formulation

From the general damage field formulation (3) and the previous section, we can readily formulate the problem of the beam equilibrium in the variational framework. Considering a distributed load $p_t(z)$ whose potential energy is $\mathcal{P} = \int p_t w$, we get the regularized energy of the solid from the previous subsection. The singular term is approximated by a convex function of the damage fields and their gradient similar to [7,10]:

$$\mathcal{E}(w, h^+, h^-) = \int_0^L \frac{EI(h^+, h^-)}{2} w_{,zz}^2 - p_t(z)w\,\mathrm{d}z$$
$$+ Gbh \int_0^L \frac{1}{4\ell}\left(\left(\frac{h^+}{h}\right)^2 + \left(\frac{h^-}{h}\right)^2\right) + \ell\left(\left(\frac{h_{,z}^+}{h}\right)^2 + \left(\frac{h_{,z}^-}{h}\right)^2\right)\,\mathrm{d}z. \tag{18}$$

The independence of the evolution of the two crack fronts on both sides of the beam is reflected in each term being independently squared. Note that this formulation of the energy is consistent with our convention for the value of h^+, h^-: the first part of the second line term is minimal when $h^+ = h^- = 0$. A dependence on a scale parameter ℓ is introduced to control the length over which the fields vary. Decreasing ℓ effectively favors sharp variations of the section.

Despite constraining the evolution of cracks to follow the beam slicing into sections as per the Euler–Bernoulli hypothesis, the whole geometry of the beam and the cracks path is specified through h^+, h^-. In practice, given a load $p_t(z)$ we look for a displacement field w and fields h^+, h^- minimizing the energy (18). From now on and for all the remaining of this paper we will assume the beam to have a straight initial shape and an initial rectangular cross-section as per the calculations of Sect. 2.1. Further we restrict ourselves to proportional loads $p_t(z) = tp(z)$.

3.2 Computing the evolution

This section is devoted to the method of computation of the unknown fields h^+, h^-, w following a quasistatic increase of the load p_t and with initial fields h_0^+, h_0^-, w_0 provided. The computation of the whole evolution roots in a time-stepping procedure. The load is discretized following instants $t_n = n\delta t$, and the fields are computed from the previous solutions. We use the staggered scheme introduced in [29] ensuring a robust and reliable resolution of the equations. The displacement field and the damage fields are computed at two different steps. We will denote w_n, h_n^+, h_n^- the unknown fields at time step t_n.

The solution unknown fields have to satisfy the stationarity equations for the functional defined (18). Following the operator split, we look at the stationarity equations for the displacement field w_n and the geometric fields h_n^+, h_n^- separately.

At time $t_n, n \geq 1$ the first step of the staggered scheme is to compute the solution displacement w_n given the value of fields h_{n-1}^+, h_{n-1}^-. The solution transversal displacement field w_n is searched as a minimizer of the restricted functional $\mathcal{E}(\cdot, h_{n-1}^+, h_{n-1}^-)$. Satisfying the Euler equation for the functional on the interior of the interval where the displacement is defined $(0, L)$:

$$\left(EI(h_{n-1}^+, h_{n-1}^-)w_{n,zz}\right)_{,zz} - p_{t_n}(z) = 0. \tag{19}$$

Providing boundary conditions suited to any problem at hand ensures well-posedness for the two point linear boundary value problem for the displacement field w_n. Boundary conditions will be specified within the examples in Sect. 4.

The second step of the staggered scheme is to solve for the geometric fields h_n^+, h_n^-. The resolution is much more delicate than for the damage fields, as the problems are highly nonlinear and constraints have to be taken into account. The system of boundary value problems is deduced from setting the first variation of the functional (18) to be zero and is supplemented with the natural boundary conditions for the fields h_n^+, h_n^-, namely:

$$h_{n,z}^+(0) = h_{n,z}^+(L) = 0, \tag{20}$$
$$h_{n,z}^-(0) = h_{n,z}^-(L) = 0. \tag{21}$$

Note that the subordination of the geometric fields evolution to the curvature sign is enforced here: depending on the geometric field considered and the sign of the beam curvature $w_{n,zz}$, the stationarity equation has to be adapted. Precisely, if the curvature sign $w_{n,zz}(z)$ is positive on some given interval (z_0, z_1), then the field $h_n^+(z)$ has to satisfy the Euler equation for the functional $\mathcal{E}(w_n, \cdot, h_n^-)$ on that interval (z_0, z_1), whereas h_n^- has to remain constant. If the curvature is negative, then it is h_n^- that has to satisfy the stationarity equations whereas h_n^+ is prescribed to be constant.

In addition, constraints on the fields value have to be satisfied as given in (??) to ensure that the section reduction due to the damage remains coherent with the initial geometry of the beam. Finally, the *Unilateral Stationarity* constraint [2] is enforced by requiring that for all n, all $0 \leq z \leq L$:
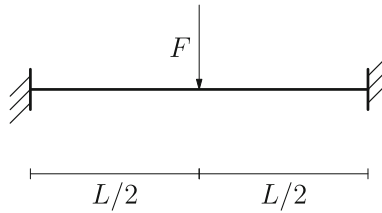
$$h_{n-1}^+(z) \leq h_n^+(z), \tag{22}$$
$$h_{n-1}^-(z) \leq h_n^-(z). \tag{23}$$

The damage is irreversible, and cracks can only open further as the load increases.

4 Examples

We investigate the predicted crack development with our model. For this purpose we compare the prediction of our unidimensional reduced model with the predictions of a finite element implementation of the variational theory [30].

Fig. 2 The clamped-clamped beam mechanical model
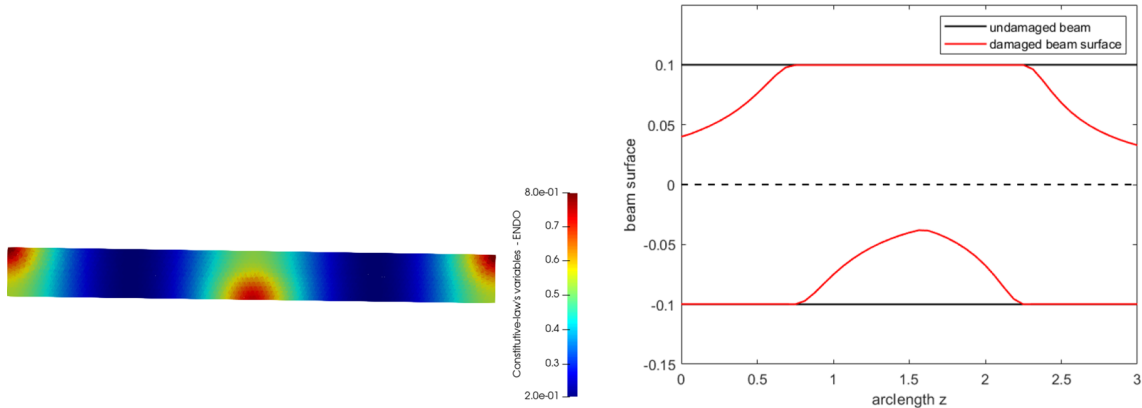
Fig. 3 Numerical results for the clamped-clamped beam. On the left, the results of the simulation with the regularized damage field model (3). On the right, the predicted cracks envelope with the geometric fields model (18). Parameters used $L = 3\,m$, $h = b = 0.2\,m$, $E = 30\,MPa$, $G = 1e^{-6}\,Nm^{-2}$, $\ell = 1e^{-5}$, $F = 4e^3\,kN$. The FE simulation is performed in CODE_ASTER using the ENDO_SCALAIRE material law with parameters $K = 0.0315$, $M = 10.0$, $P = 5.0$ and a characteristic length $0.6\,m$

4.1 Clamped-clamped beam

The first load case we investigate is that of a beam whose two ends are clamped, loaded in the middle of its span with a single point force F. The mechanical model can be seen in Fig. 2. The boundary condition for the associated model are the geometrical conditions on the beam centre-line:

$$w(0) = w(L) = 0, \tag{24}$$

$$w_{,z}(0) = w_{,z}(L) = 0. \tag{25}$$

Namely there is no transversal displacement for the beam centre line at the clamped points, and the centre-line of the beam there is horizontal. The results of the resolution following the algorithm of Sect. 3.2 are shown in Fig. 3.

The moment diagram for the mechanical model of Fig. 2 when the beam section is kept constant has three extrema at the extremal and middle points of the beam $z = 0$, $z = L/2$, $z = L$. On the left of Fig. 3, the damage field obtained after a gradual load increase is showed. The zones of large damage are figured in red. As expected, fracture initiate at the 3 points of maximal strain: on the tensiled, top parts of the beam at the supports $z = 0$, $z = L$, and bottom part at the midpoint $z = L/2$. On the right hand side of the figure, the original shape of the beam is figured in black and the damaged surface of the beam in red. The essential features of the cracking pattern are grasped through the dimension reduction: the shape of the damage zone obtained through the two-dimensional damage field model matches that of the depth crack penetration on the right. On the other hand, our model predicts a strong smearing of the damage despite our small characteristic length. Neglecting the effect of the crack on the stress distribution induces a diffusion of the damage farther away from the point maximal moment.

4.2 Two points loaded cantilever beam

The second load case we investigate is that of a simple cantilevered beam loaded in the middle and the end of its span with single point forces F_1, F_2. The mechanical model is given in Fig. 4. The boundary conditions to
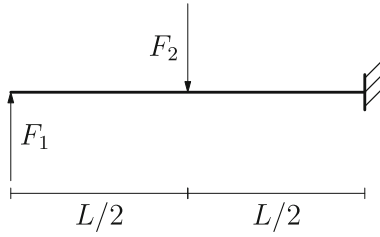
Fig. 4 The cantilever loaded with two point loads mechanical model
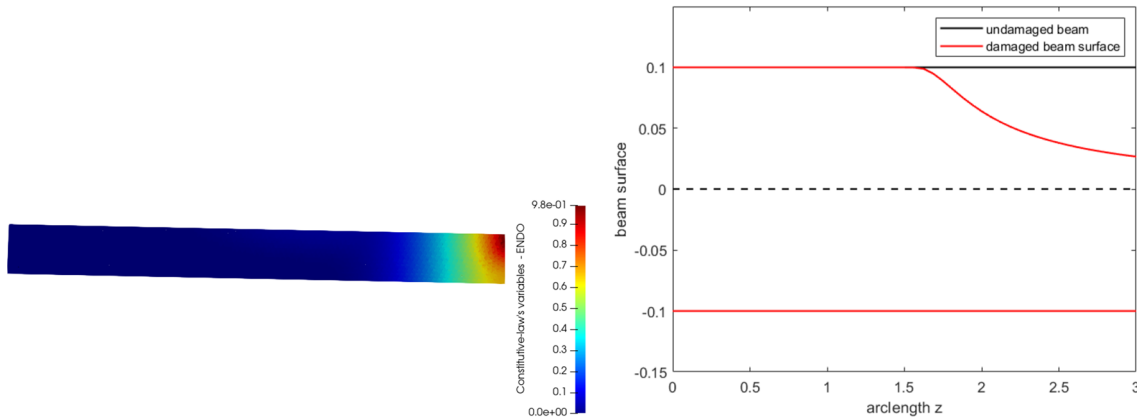
Fig. 5 Numerical results for the clamped-clamped beam. On the left, the results of the simulation with the regularized damage field model (3). On the right, the predicted cracks envelope with the geometric fields model (18). Parameters used $L = 3\,m$, $h = b = 0.2\,m$, $E = 30\,MPa$, $G = 1e^{-6}\,Nm^{-2}$, $\ell = 1e^{-5}\,m$, $F_1 = F_2 = 1e^3\,kN$. The FE simulation is performed in CODE_ASTER using the ENDO_SCALAIRE material law with parameters $K = 0.0315$, $M = 10.0$, $P = 5.0$ and a characteristic length $0.6\,m$

associate are the following

$$w(L) = 0, w_{,z}(L) = 0, \tag{26}$$
$$w_{,zz}(0) = 0, w_{,zzz}(0) = 0. \tag{27}$$

That is, the transversal displacement and the angle of the centre line with the horizontal are prescribed to be zero at the attach point $z = L$, whereas the centre-line curvature and its derivative are zero at the free end.

As we investigate the case where $F1 = F2$, the moment diagram for the mechanical model of Fig. 4, computed with the Euler–Bernoulli hypothesis has two maxima at $z = L/2$, $z = L$. The solution obtained by the damage field model is given in Fig. 5 left, with the most damaged zones in red. The damage concentrates on the tensiled side of the beam at the attach point, initiating at the point of maximal moment. The damaged zone expands far away from the support with our model, probably for the same reason as in Sect. 4.1. Nonetheless the appearance point of the crack at the support matches in both simulation.

5 Discussion and results

The envelope of the cracks appearing in a beam under flexion was computed using a dimension reduction method. Under plane displacement assumptions, we adopted a parametrization of the beam section geometry at any arclength, allowing for the description of the stress fields in the beam and computation of the stress resultants by direct integration. Completing the formulation by the addition of a regularizing term in the energetic formulation leads to predict cracks initiation at finite loads.

The position of the cracks appearance zone is found to match those of the usual engineering stress criterion, and smeared, crack zones appear at positions of maximal bending moment in the undamaged configuration. The smearing of the cracks can be related to the shortcomings of the crack modeling in our model, which accurately represents the geometry of the section, but does not phenomenologically represent cracks. In particular, and in opposition to sharp cracks representation, the stress resultants do not exhibit jumps at cracking points.

In the present model, stress relaxation due to cracking only occurs through local reduction of the section's moment of inertia, whereas the appearance of a strong singularity at the crack tip should modify the stress fields within the beam depth. Nonetheless, the model predicts crack initiation at a finite load so long as the crack occupies some non-zero measure part of the beam, what is adequately enforced by the use of a regularized field. The points of crack initiation can be evaluated together with the initial crack depth, and the behavior of beams developing multiple cracks could be investigated by placing discrete elements accurately representing cracks behavior at points of expected cracks initiation.

Declarations

Conflict of interest The author has no interest to declare that are relevant to the content of this article.

References

1. Griffith, A.A.: VI The phenomena of rupture and flow in solids. Philos. Trans., R Soc. Lond. Ser. A 221(582-593), 163-198 (1921)
2. Bourdin, B., Francfort, G.A., Marigo, J.J.: The variational approach to fracture. J. Elast. **91**, 5–148 (2008)
3. Chambolle, A., Giacomini, A., Ponsiglione, M.: Crack initiation in brittle materials. Arch. Ration. Mech. Anal. **188**(2), 309–349 (2008)
4. Kumar, A., Bourdin, B., Francfort, G.A., Lopez-Pamies, O.: Revisiting nucleation in the phase-field approach to brittle fracture. J. Mech. Phys. Solids **142**, 104027 (2020)
5. Tanné, E., Li, T., Bourdin, B., Marigo, J.J., Maurini, C.: Crack nucleation in variational phase-field models of brittle fracture. J. Mech. Phys. Solids **110**, 80–99 (2018)
6. Ambrosio, L., Tortorelli, V.M.: Approximation of functional depending on jumps by elliptic functional via t- convergence. Commun. Pure Appl. Math. **43**(8), 999–1036 (1990)
7. Bourdin, B., Chambolle, A.: Implementation of an adaptive finite-element approximation of the Mumford-Shah functional. Numer. Math. **85**, 609–646 (2000)
8. Del Piero, G.: A variational approach to fracture and other inelastic phenomena. J. Elast. **112**, 3–77 (2013)
9. Freddi, F., Royer-Carfagni, G.: Regularized variational theories of fracture: a unified approach. J. Mech. Phys. Solids **58**(8), 1154–1174 (2010)
10. Miehe, C., Welschinger, F., Hofacker, M.: Thermodynamically consistent phase- field models of fracture: Variational principles and multi- field FE implementations. Int. J. Numer. Meth. Eng. **83**(10), 1273–1311 (2010)
11. Amor, H., Marigo, J.J., Maurini, C.: Regularized formulation of the variational brittle fracture with unilateral contact: Numerical experiments. J. Mech. Phys. Solids **57**(8), 1209–1229 (2009)
12. Ambati, M., Gerasimov, T., De Lorenzis, L.: A review on phase-field models of brittle fracture and a new fast hybrid formulation. Comput. Mech. **55**, 383–405 (2015)
13. Michel, S., Sipos, A.A.: On the cracking patterns of brittle rings with elastic radial support under hydrostatic pressure. Meccanica **57**(7), 1639–1656 (2022)
14. Michel, S., Sipos, A.A.: Fragmentation of inflated elastic brittle rings: Emergence of the quasi-equidistant spacing of cracks. J. Mech. Phys. Solids, 105372 (2023)
15. Bažant, Z.P.: Scaling of quasibrittle fracture: asymptotic analysis. Int. J. Fract. **83**, 19–40 (1997)
16. Christides, S., Barr, A.D.S.: One-dimensional theory of cracked Bernoulli-Euler beams. Int. J. Mech. Sci. **26**(11–12), 639–648 (1984)
17. Maier, G., Zavelani, A., Dotreppe, J.C.: Equilibrium branching due to flexural softening. J. Eng. Mech. Div. **99**(4), 897–901 (1973)
18. Thomson, W.T.: Vibration of slender bars with discontinuities in stiffness. J. Appl. Mech. **16**(2), 203–207 (1949)
19. Caddemi, S., Morassi, A.: Multi-cracked Euler-Bernoulli beams: mathematical modeling and exact solutions. Int. J. Solids Struct. **50**(6), 944–956 (2013)
20. Donà, M., Palmeri, A., Lombardo, M.: Exact closed-form solutions for the static analysis of multi-cracked gradient-elastic beams in bending. Int. J. Solids Struct. **51**(15–16), 2744–2753 (2014)
21. Kiendl, J., Ambati, M., De Lorenzis, L., Gomez, H., Reali, A.: Phase-field description of brittle fracture in plates and shells. Comput. Methods Appl. Mech. Eng. **312**, 374–394 (2016)

22. Amiri, F., Millán, D., Shen, Y., Rabczuk, T., Arroyo, M.: Phase-field modeling of fracture in linear thin shells. Theoret. Appl. Fract. Mech. **69**, 102–109 (2014)
23. Ulmer, H., Hofacker, M., Miehe, C.: Phase field modeling of fracture in plates and shells. PAMM **12**(1), 171–172 (2012)
24. Areias, P., Rabczuk, T., Msekh, M.: Phase-field analysis of finite-strain plates and shells including element subdivision. Comput. Methods Appl. Mech. Eng. **312**, 322–350 (2016)
25. Lai, W., Gao, J., Li, Y., Arroyo, M., Shen, Y.: Phase field modeling of brittle fracture in an Euler-Bernoulli beam accounting for transverse part-through cracks. Comput. Methods Appl. Mech. Eng. **361**, 112787 (2020)
26. Corsi, G., Favata, A., Vidoli, S.: A coarse-grained constitutive law for fracturing beams based on a sharp interface crack representation. Int. J. Solids Struct. 112224 (2023)
27. Lancioni, G., Royer-Carfagni, G.: The variational approach to fracture mechanics. A practical application to the French Panthéon in Paris. J. Elast. **95**, 1–30 (2009)
28. Marconi, V.I., Jagla, E.A.: Diffuse interface approach to brittle fracture. Phys. Rev. E **71**(3), 036110 (2005)
29. Miehe, C., Hofacker, M., Welschinger, F.: A phase field model for rate-independent crack propagation: robust algorithmic implementation based on operator splits. Comput. Methods Appl. Mech. Eng. **199**(45–48), 2765–2778 (2010)
30. Electricité de France, Finite element *code_aster*, Analysis of Structures and Thermomechanics for Studies and Research, *Open source on www.code-aster.org*, 1989–2023
31. Bourdin, B.: Numerical implementation of the variational formulation for quasi-static brittle fracture. Interfaces Free Bound. **9**(3), 411–430 (2007)